

# Evidence for a new phase of dense hydrogen above 325 gigapascals

Philip Dalladay-Simpson<sup>1</sup>, Ross T. Howie<sup>1†</sup> & Eugene Gregoryanz<sup>1,2</sup>

Almost 80 years ago it was predicted that, under sufficient compression, the H–H bond in molecular hydrogen (H<sub>2</sub>) would break, forming a new, atomic, metallic, solid state of hydrogen<sup>1</sup>. Reaching this predicted state experimentally has been one of the principal goals in high-pressure research for the past 30 years. Here, using *in situ* high-pressure Raman spectroscopy, we present evidence that at pressures greater than 325 gigapascals at 300 kelvin, H<sub>2</sub> and hydrogen deuteride (HD) transform to a new phase—phase V. This new phase of hydrogen is characterized by substantial weakening of the vibrational Raman activity, a change in pressure dependence of the fundamental vibrational frequency and partial loss of the low-frequency excitations. We map out the domain in pressure–temperature space of the suggested phase V in H<sub>2</sub> and HD up to 388 gigapascals at 300 kelvin, and up to 465 kelvin at 350 gigapascals; we do not observe phase V in deuterium (D<sub>2</sub>). However, we show that the transformation to phase IV' in D<sub>2</sub> occurs above 310 gigapascals and 300 kelvin. These values represent the largest known isotropic shift in pressure, and hence the largest possible pressure difference between the H<sub>2</sub> and D<sub>2</sub> phases, which implies that the appearance of phase V of D<sub>2</sub> must occur at a pressure of above 380 gigapascals. These experimental data provide a glimpse of the physical properties of

dense hydrogen above 325 gigapascals and constrain the pressure and temperature conditions at which the new phase exists. We speculate that phase V may be the precursor to the non-molecular (atomic and metallic) state of hydrogen that was predicted 80 years ago.

The exchange interaction, a purely quantum mechanical effect, forms one of the strongest bonds in chemistry—the H–H bond. Owing to this bond, hydrogen exists in molecular form, with atoms separated by approximately 0.74 Å and a bond dissociation energy of approximately 4.52 eV (refs 2, 3) at ambient conditions. The first experiments to break this bond<sup>4</sup> demonstrated that extreme conditions are needed to do so; for example, the H<sub>2</sub> molecule dissociates only to a minor extent at high temperatures (at 3,000 K, the degree of dissociation is around 10%)<sup>5</sup>. Another mechanism to break the hydrogen bond—pressure—was subsequently proposed<sup>1</sup>; it was theorized that above 250,000 atm (25 GPa), the hydrogen molecules would dissociate, forming solid, atomic, metallic hydrogen, an entirely new state of the first and simplest element.

The proposed high-pressure route to an atomic metallic state has proved to be one of the great experimental challenges in high-pressure physics. Despite the technological advances in high-pressure physics, this theoretical prediction has yet to be experimentally confirmed, even

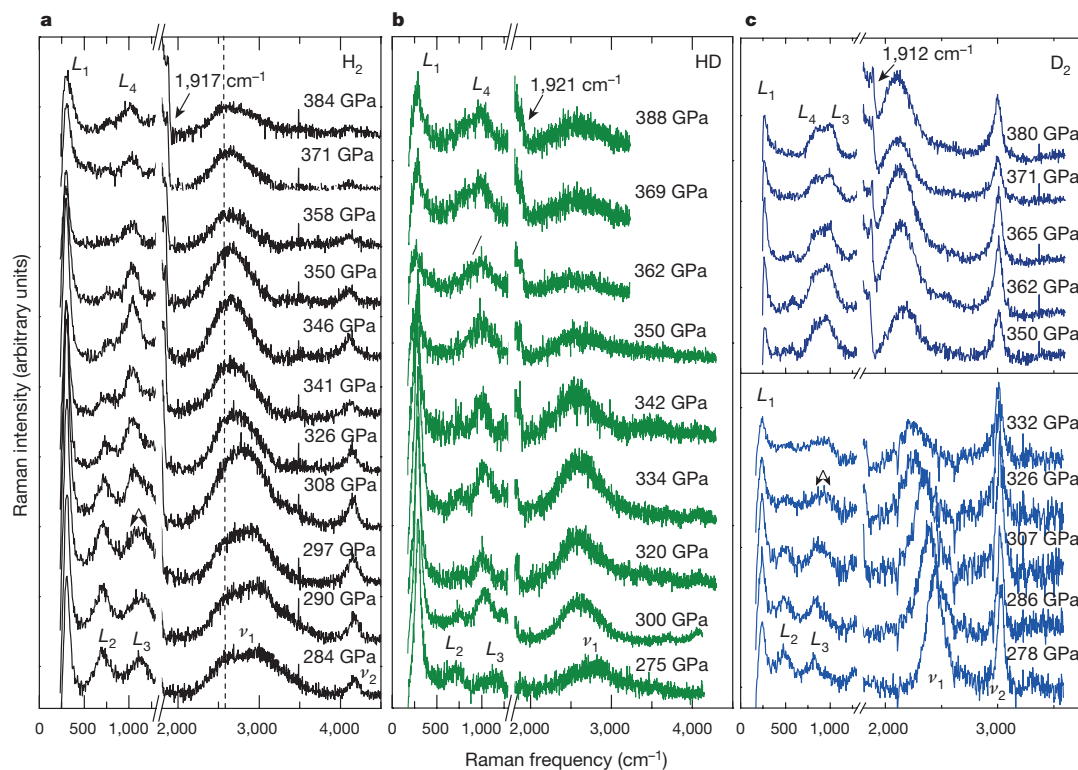


**Figure 1 | Representative Raman spectra of three hydrogen isotopes.** a–c, Spectra of hydrogen are shown in black (a), hydrogen deuteride in green (b) and deuterium in blue (c). The spectra at different pressures (as labelled) are plotted as a waterfall; the offset is for clarity. The low-frequency modes  $L_{1-4}$  and the vibrational modes  $\nu_{1,2}$  are labelled. The second-order diamond band spanning 2,300–2,600  $\text{cm}^{-1}$  is visible on some spectra; its central position is marked by the dashed vertical line in a. The diamond edge for each isotope, which was used to determine the pressure, is labelled on the highest-pressure spectra (1,917  $\text{cm}^{-1}$  for H<sub>2</sub>, 1,921  $\text{cm}^{-1}$  for HD and 1,912  $\text{cm}^{-1}$  for D<sub>2</sub>). HD was formed from a mixture of H<sub>2</sub> (75%) and D<sub>2</sub> (25%); see Methods. The spectra were collected using a 647.1-nm excitation wavelength. The arrows in a and c represent the splitting of the L<sub>3</sub> mode and the onset of IV' (for clarity see Extended Data Fig. 4).

<sup>1</sup>School of Physics and Centre for Science at Extreme Conditions, University of Edinburgh, Edinburgh EH9 3JZ, UK. <sup>2</sup>Key Laboratory of Materials Physics, Institute of Solid State Physics, Chinese Academy of Sciences, Hefei 230031, China. †Present address: Center for High Pressure Science & Technology Advanced Research, Shanghai 201203, China.

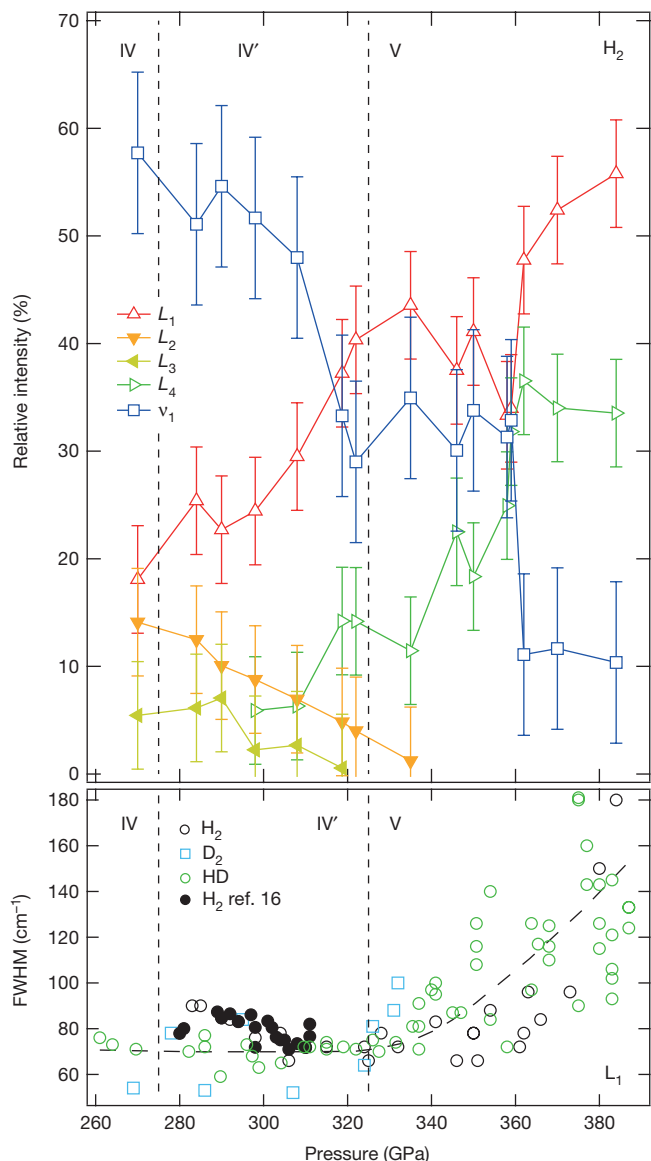


**Figure 2 | Relative intensities of the vibrational, low-frequency modes and the full-width at half-maximum of the  $L_1$  mode as a function of pressure.** **a**, Relative intensities of the vibrational ( $\nu_1$ ) and four low-frequency modes ( $L_{1-4}$ ) of hydrogen represented as a percentage of the total Raman activity of the sample; error bars reflect the accuracy of the measurement (see Methods and Extended Data Fig. 7). The low-frequency modes  $L_2$  and  $L_3$  disappear at around 325 GPa. **b**, The full-width at half-maximum (FWHM) of the low-frequency mode  $L_1$  of  $H_2$ ,  $D_2$  and HD as function of pressure; the dashed curve is a guide to the eye. The dashed vertical lines in **a** and **b** indicate the transformations to phases IV' and V.

at pressures (and high temperatures) an order of magnitude higher than that originally proposed<sup>6–14</sup>. Recently, a new solid phase of dense hydrogen—phase IV—was experimentally discovered<sup>15,16</sup> at 300 K and above 230 GPa. This new phase IV exhibits a change in the gradient of the fundamental vibrational-mode frequency  $\nu_1$  with respect to pressure  $P$  at a constant temperature  $T = 300$  K,  $(d\nu_1/dP)_T$ , which leads to extremely low values of  $\nu_1$  above 230 GPa; for example,  $\nu_1 \approx 2,750$   $\text{cm}^{-1}$  at 315 GPa (ref. 16). This value is indicative of a much weaker bond, compared to ambient conditions, and is consistent with the bond length of approximately 0.82 Å (ref. 17). It was observed that phase IV could be viewed as a mixed molecular and atomic state and that the complete dissociation of the hydrogen molecule is feasible at even higher compressions<sup>18</sup>.

To investigate the states of hydrogen above 320 GPa, we conducted very high pressure studies on  $H_2$ , HD (hydrogen deuteride) and  $D_2$ ,

reaching pressures of  $384 \pm 15$  GPa,  $388 \pm 15$  GPa and  $380 \pm 15$  GPa, respectively. These pressures, despite being conservative estimates (see Methods and Extended Data Figs 1 and 2), are still among the highest pressures reported so far in a diamond anvil cell, and the highest pressures hydrogen has so far been subjected to in static experiments. On the basis of the substantial decrease in intensity of vibrational Raman bands, the change of slope of the vibrational-mode frequency with pressure, and changes in position, width and intensity of the low-frequency ( $<1,300$   $\text{cm}^{-1}$ ) modes, we tentatively infer a transition to a new structural configuration—phase V—of  $H_2$  and HD above 325 GPa, while observing phase IV' of  $D_2$  above 310 GPa. We present experimental information on the physical properties of the dense hydrogen just below 400 GPa and provide some constraints on the  $P$ - $T$  space of phase V. On the basis of the optical changes observed through the phase transition, we speculate that the proposed phase V might be the onset of a non-molecular state of hydrogen.

Figure 1 shows the representative Raman spectra of three isotopes of hydrogen compressed at 300 K. (For the full description of the relevant experimental details, see Methods and refs 18 and 19; further information about the intensities of the modes and frequencies of HD as a function of H/D concentration and pressure is provided in ref. 20.) Above 220 GPa, all hydrogen isotopes enter phase IV, which is characterized by sharp, well-defined, low-frequency modes (Fig. 1, marked for clarity as  $L_1$ ,  $L_2$  and  $L_3$  in all figures; see also ref. 20) and the presence of a second vibrational fundamental mode  $\nu_2$ . The appearance of the Raman spectra of HD (at similar pressures) is essentially identical to those of  $H_2$  or  $D_2$  (refs 16, 18); see Extended Data Fig. 3. When pressures above 275 GPa are reached (for  $H_2$  and HD), we observe a change in the gradient of the frequency with respect to pressure of the  $L_3$  mode, and its branching to produce a new  $L_4$  mode. These changes mark the appearance of phase IV', described previously<sup>18</sup>. It was suggested that phase IV' could structurally resemble phase IV, on the basis of close similarities between the Raman spectra<sup>18</sup>. Above 320 GPa we observe gradual, but profound, modification in the Raman spectra, indicative of the phase transformation to a new phase, phase V ( $H_2$  and HD only). The pressure needed to enter phase IV' in deuterium is 35 GPa higher, as evidenced by the splitting of  $L_3$  into  $L_3$  and  $L_4$  at 310 GPa (Fig. 1, Extended Data Fig. 4).

In hydrogen, after branching to produce the  $L_4$  mode, the  $L_3$  mode slowly redistributes its intensity into the  $L_4$  mode (Figs 1, 2 and Extended Data Fig. 4). When the suggested phase V is reached, the  $L_3$  mode completely disappears and the intensity of  $L_4$  becomes comparable to that of the  $L_1$  mode (Figs 1 and 2). Meanwhile, the  $L_1$  mode undergoes a marked change itself; Fig. 2b shows the full-width at half-maximum (FWHM) of  $L_1$  as function of pressure. At the same pressure as when the vibrational Raman modes start to become weaker and the  $L_2$  and  $L_3$  modes disappear ( $>325$  GPa; see Figs 1 and 2), the FWHM of the  $L_1$  mode starts to increase rapidly. Between 330 GPa and 388 GPa the width of the  $L_1$  mode increases more than twofold, reaching 180  $\text{cm}^{-1}$  by 388 GPa (Fig. 2b). Even though the  $L_1$  mode is very broad at the highest pressures, it remains the dominant feature of the spectra of all isotopes (Fig. 1). We also observe some small but detectable softening of the  $L_1$  frequency with pressure (Fig. 3).

Up to 325 GPa, the total Raman intensity of all modes stays roughly the same (Fig. 2) for all three isotopes, in agreement with previous studies<sup>16</sup> of pure  $H_2$  up to 315 GPa. However, when pressures above 325 GPa are reached, the low-frequency modes  $L_2$  and  $L_3$  disappear and the intensities of both vibrational excitations of  $H_2$  and HD start to decrease rapidly. In the case of hydrogen, the  $\nu_2$  modes become almost indistinguishable from the background above 358 GPa, whereas the  $\nu_1$  mode becomes broad and weak, overlapping with the second-order diamond band (Fig. 1a); the positions of the hydrogen and deuterium vibrational modes are clearly visible in all spectra (Fig. 1). The second-order diamond mode spanning the approximate range 2,300–2,600  $\text{cm}^{-1}$  overlaps in frequency with the  $\nu_1$  mode of all isotopes,

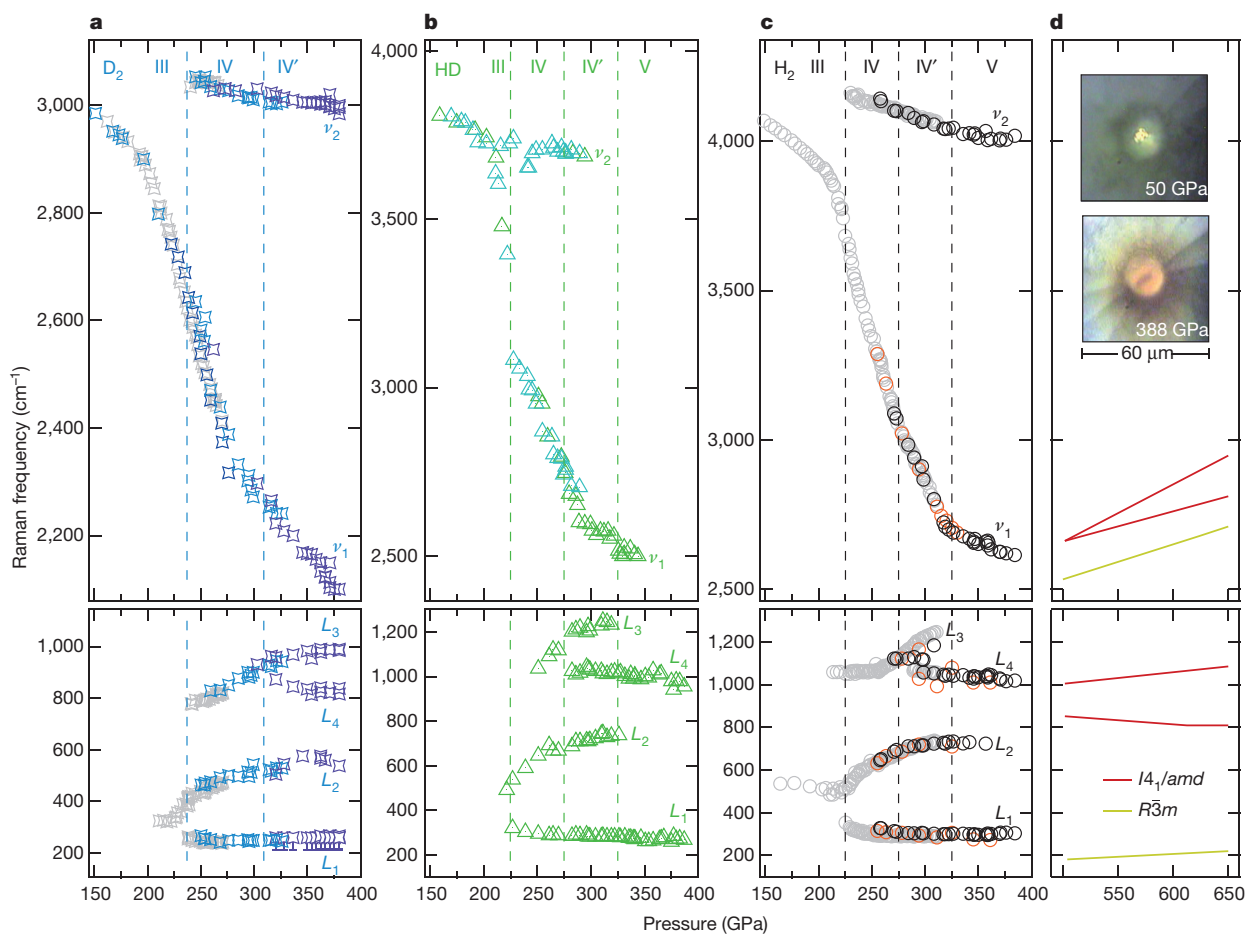


**Figure 3 | Frequencies of the vibrational and low-energy modes of the isotopes as functions of pressure.** **a–c.** The data for the different isotopes are shown as open stars ( $D_2$ ; **a**), triangles with centre dots (HD; **b**) and open circles ( $H_2$ ; **c**), with different colours representing different experimental runs. Data from previous studies<sup>16,18</sup> are shown as grey symbols. The vertical dashed lines denote the phase transitions in the

which makes the estimation of its intensity difficult. In the case of HD, it became impossible to distinguish between the second-order diamond mode and the  $\nu_1$  mode above 350 GPa (Fig. 1b). The notable decrease of the vibrational-mode intensity means that the spectra of the suggested phase V looks highly unusual, particularly when compared with those of phase IV, in which the vibrational mode dominates (see >270–320-GPa spectra of all isotopes in Fig. 1). As well as the pronounced drop of the intensities of the vibrational modes, we observe a change in the slope of the  $\nu_1$  frequency with pressure ( $d\nu_1/dP$ )<sub>T</sub> at around 325 GPa for hydrogen and hydrogen deuteride (Fig. 3). The  $\nu_1$  mode softens rapidly with pressure in phase IV (average gradient of  $-12 \text{ cm}^{-1} \text{ GPa}^{-1}$ ; ref. 16) and changes to a rate of about  $-7 \text{ cm}^{-1} \text{ GPa}^{-1}$  (refs 16, 18) in phase IV'. When hydrogen is compressed to more than 325 GPa, the softening of the  $\nu_1$  mode essentially stops and ( $d\nu_1/dP$ )<sub>T</sub> becomes almost independent of pressure (equal to  $-1.37 \text{ cm}^{-1} \text{ GPa}^{-1}$ ), resembling that of the  $\nu_2$  mode ( $-1.01 \text{ cm}^{-1} \text{ GPa}^{-1}$ ); see Fig. 3. The change of slope and the sudden increase of the FWHM of the  $L_1$  mode happen at the same pressure, suggesting that the nature of the bonding is noticeably modified by the transition between phase IV(IV') and V'. In a recent Raman optical study<sup>21</sup>, a small change in the slope of the vibrational mode of the  $H_2$  vibrational mode at 300 GPa was observed, from which three structural phase transitions within 50 GPa (275–325 GPa) were inferred. However, our data do not seem to support these findings (Extended Data Fig. 5).

The pressure at which phase IV of deuterium appears is about 10 GPa higher than that of hydrogen<sup>18</sup>, whereas the transition from phases IV

corresponding isotope. **d.** The theoretically calculated frequencies of hydrogen for the metallic and non-molecular (atomic) structures of  $I4_1/amd$  (red) and  $R\bar{3}m$  (yellow) from ref. 22. The insets are photos of the HD sample at 50 GPa and at 388 GPa, as labelled, taken in transmitted and reflected light.

to IV' is shifted by 35–40 GPa. We observe similar qualitative changes in the slope of the deuterium vibrational mode at 310 GPa upon entrance into phase IV', but the slope remains relatively steep, resulting in the extremely low vibrational frequency of approximately  $2,100 \text{ cm}^{-1}$  at 380 GPa. The large pressure difference between phase IV' of hydrogen and that of deuterium suggests that phase V of deuterium will appear at pressures above 380 GPa.

We investigated the  $P$ – $T$  space where phase IV(IV') and the proposed phase V exist by conducting heating experiments. If hydrogen is heated at 250 GPa, then the phase IV  $\leftrightarrow$  I transformation happens at 430 K, and at 450 K phase I presumably melts (see Fig. 4 and the figures in ref. 14). In some runs, phase IV(IV') was heated at pressures above the I–IV–liquid<sup>14</sup> triple point—for example, at 262 GPa to approximately 450 K and at 270 GPa and 290–310 GPa to approximately 375 K—but no transformations to phase V were observed (Fig. 4). Finally, we heated phase V at 350 GPa and did not observe any transformation up to 465 K (Extended Data Fig. 6). These points in  $P$ – $T$  space indicate that phase V is separated from the lower-pressure phase IV(IV') by a phase line that is probably close to vertical (Fig. 4).

The decrease in the vibrational-mode intensities could indicate the loss of sample, particularly in the case of hydrogen, but the observations described above rule this out and instead indicate a possible phase transition. These observations include: the evolution of the low-frequency modes (that is, broadening and frequency change) with pressure up to 390 GPa, and only a modest drop in the intensity of the  $L_1$  mode; the noticeable change in the slope of the vibrational-mode

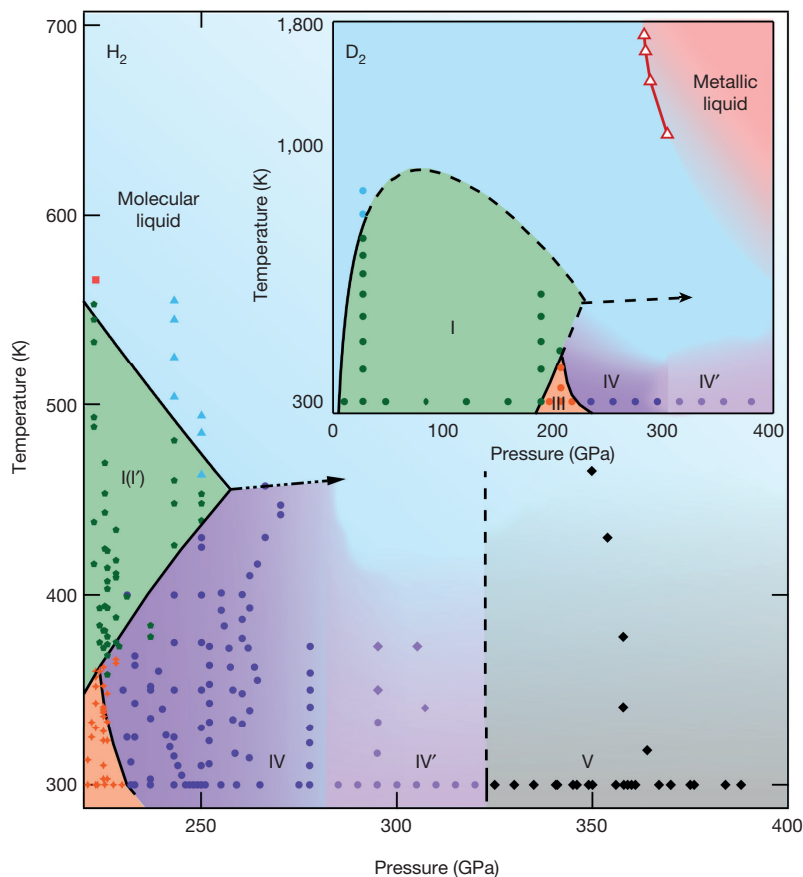


**Figure 4 | Proposed phase diagram of hydrogen up to 400 GPa.** The coloured, filled symbols and solid phase lines below 300 GPa in the main figure are from ref. 14, and show phases I(I'), III and IV(IV'). The solid black diamonds (phase V) are from this study, the vertical, grey dashed line indicates the transition from phase IV' to phase V and the dashed-dotted arrow is the proposed continuation of the melting curve. The inset shows a sketch of the phase diagram of D<sub>2</sub>. The coloured, filled symbols and solid lines were obtained by us in another, unreported study. The dashed lines are the proposed melting curves of deuterium, which have not been measured experimentally, but are assumed to follow the same trend as those of hydrogen. The red open triangles are from ref. 26 and separate the metallic and semi-conducting liquids.

frequency with pressure at 325 GPa at 300 K; and the lack of sample loss or detection of transformation upon heating at pressures above 320 GPa. In heating experiments, rapid sample loss is observed in the liquid state, which results in the complete disappearance of all hydrogen Raman activity and the resulting spectra resemble those of the gasket (Extended Data Fig. 6).

It is tempting, although highly speculative at this time, to interpret phase V as the onset of the predicted<sup>1</sup> non-molecular and metallic state of hydrogen. *Ab initio* random-structure searches that included zero-point motion estimate that hydrogen should dissociate into atomic and metallic states at around 500 GPa (ref. 22) and 380 GPa (ref. 23), respectively. The possible lowest-energy structural candidates include the tetragonal  $I4_1/amd$  and trigonal  $R\bar{3}m$  symmetries<sup>22,23</sup>. Both structures have inter-atomic Raman phonons with frequencies of about  $2,500\text{ cm}^{-1}$  at 500 GPa, which is close to the frequency of the vibrational mode  $\nu_1$  of hydrogen that we observe at 380 GPa (see Fig. 3 and supplementary information in ref. 22). In calculations, these phonons are present up to 4.2 TPa, slowly increasing in energy with increasing pressure<sup>22</sup> as the distance between the atoms decreases. The presence of the extremely weak  $\nu_2$  mode at 384 GPa (Fig. 1a) indicates that the purely atomic state was not reached in our experiments and that slightly higher pressures are required to completely dissociate hydrogen. It is plausible that the molecular dissociation commences at pressures above 350 GPa, resulting in the alterations of the Raman spectrum as described here. If the suggested phase V is indeed the beginning of the complete molecular dissociation of partially molecular phase IV', then it could explain all the optical observations presented here, such as the band gap decreasing with pressure (1.8 eV at 315 GPa in phase IV', ref. 16). Furthermore, the possible appearance of conducting electrons due to dissociation could explain the very dark appearance of the sample as seen in transmitted and reflected light in the visible region (Fig. 3d, inset), and the overall decrease of the Raman intensities. The relatively simple overall Raman spectrum observed experimentally matches those predicted theoretically rather well (Fig. 3d). The  $I4_1/amd$

symmetry does not predict a very prominent  $L_1$  mode, whereas the  $R\bar{3}m$  symmetry, which is more energetically favourable at even higher pressures, does not predict the  $L_4$  mode (see Fig. 3b, c), both of which are observed experimentally. However, these discrepancies could be accounted for by the 100-GPa pressure difference between theory and experiment. A minimum in  $(d\nu_1/dP)_T$  would indicate the evolution from the intramolecular vibrational mode to an interatomic phonon. This change could require a 100-GPa pressure range to complete and would result in hardening of the phonons at pressures above 500 GPa.

The data from this and a previous melting study<sup>14</sup> provide further insight into the current phase diagram of hydrogen (Fig. 4). It appears that there could be another triple point between the proposed phase V, phase IV(IV'), and a liquid state (not shown) at above 275 GPa and 450 K. If phase V is indeed a precursor to a fully non-molecular, and presumably metallic, solid state, then a question arises about the existence and location of the phase line separating the molecular (insulating) and non-molecular (metallic) liquids and solids. A non-molecular liquid could be expected to exist in the same pressure range as phase V, but at higher temperatures. In fact, theoretical studies have suggested a phase transition from a molecular liquid to an atomic liquid in hydrogen<sup>24,25</sup>. The data presented in refs 24 and 25 suggest the existence of the highly conducting atomic liquid state at pressures as low as about 150 GPa and above 2,000 K (ref. 25). However, shock-wave experiments<sup>26</sup> indicate the existence of the metallic liquid deuterium at higher pressures of 350 GPa, with the corresponding phase line being almost vertical (Fig. 4, inset). These experimental results seem to be in a very good agreement with our current study. Extrapolation of the data from ref. 26 to lower temperatures would imply yet another triple point between the melting curve and the two liquid phases. The presence of two dissimilar liquids would suggest the presence of two solid phases below them, with properties mimicking those of the liquids, for example, non-molecular (insulating) versus atomic (metallic). Experimental confirmation of the location of the phase line(s) and triple points would be very

important for the complete description of phase V, even higher-pressure solid phases and the possible molecular–atomic transition. An understanding of the connection between the proposed metallization and phase V is also required. Such additional data could provide invaluable information about the fundamental physics and chemistry that governs the behaviour of the simplest element at high densities.

**Online Content** Methods, along with any additional Extended Data display items and Source Data, are available in the online version of the paper; references unique to these sections appear only in the online paper.

**Received 16 June; accepted 14 October 2015.**

- Wigner, E. & Huntington, H. B. On the possibility of a metallic modification of hydrogen. *J. Chem. Phys.* **3**, 764–770 (1935).
- van Kranendonk, J. *Solid Hydrogen* (Plenum Press, 1983).
- Housecroft, C. E. & Sharpe, A. G. *Inorganic Chemistry* (Prentice Hall, 2007).
- Langmuir, I. & Mackay, G. M. J. The dissociation of hydrogen into atoms. Part I. Experimental. *J. Am. Chem. Soc.* **36**, 1708–1722 (1914).
- Langmuir, I. The dissociation of hydrogen into atoms. [Part II.] Calculation of the degree of dissociation and the heat of formation. *J. Am. Chem. Soc.* **37**, 417–458 (1915).
- Goncharov, A. F., Gregoryanz, E., Hemley, R. J. & Mao, H.-k. Spectroscopic studies of the vibrational and electronic properties of solid hydrogen to 285 GPa. *Proc. Natl Acad. Sci. USA* **98**, 14234–14237 (2001).
- Loubeyre, P., Occelli, F. & LeToullec, R. Optical studies of solid hydrogen to 320 GPa and evidence for black hydrogen. *Nature* **416**, 613–617 (2002).
- Gregoryanz, E., Goncharov, A., Matsuishi, K., Mao, H.-k. & Hemley, R. Raman spectroscopy of hot dense hydrogen. *Phys. Rev. Lett.* **90**, 175701 (2003).
- Eremets, M. I. & Trojan, I. A. Evidence of maximum in the melting curve of hydrogen at megabar pressures. *JETP Lett.* **89**, 174–179 (2009).
- Subramanian, N., Goncharov, A. F., Struzhkin, V. V., Somayazulu, M. & Hemley, R. J. Bonding changes in hot fluid hydrogen at megabar pressures. *Proc. Natl Acad. Sci. USA* **108**, 6014–6019 (2011).
- Akahama, Y. *et al.* Evidence from x-ray diffraction of orientational ordering in phase III of solid hydrogen at pressures up to 183 GPa. *Phys. Rev. B* **82**, 060101 (2010).
- Akahama, Y., Kawamura, H., Hirao, N., Ohishi, Y. & Takemura, K. Raman scattering and x-ray diffraction experiments for phase III of solid hydrogen. *J. Phys. Conf. Ser.* **215**, 012056 (2010).
- Zha, C.-S., Liu, Z. & Hemley, R. J. Synchrotron infrared measurements of dense hydrogen to 360 GPa. *Phys. Rev. Lett.* **108**, 146402 (2012).
- Howie, R. T., Dalladay-Simpson, P. & Gregoryanz, E. Raman spectroscopy of hot hydrogen above 200 GPa. *Nature Mater.* **14**, 495–499 (2015).
- Eremets, M. I. & Trojan, I. A. Conductive dense hydrogen. *Nature Mater.* **10**, 927–931 (2011).
- Howie, R. T., Guillaume, C. L., Scheler, T., Goncharov, A. F. & Gregoryanz, E. Mixed molecular and atomic phase of dense hydrogen. *Phys. Rev. Lett.* **108**, 125501 (2012).
- Pickard, C. J. & Needs, R. J. Structure of phase III of solid hydrogen. *Nature Phys.* **3**, 473–476 (2007).
- Howie, R. T., Scheler, T., Guillaume, C. L. & Gregoryanz, E. Proton tunneling in phase IV of hydrogen and deuterium. *Phys. Rev. B* **86**, 214104 (2012).
- Howie, R. T., Gregoryanz, E. & Goncharov, A. F. Hydrogen (deuterium) vibron frequency as a pressure comparison gauge at multi-Mbar pressures. *J. Appl. Phys.* **114**, 073505 (2013).
- Howie, R. T., Magdäu, I. B., Goncharov, A. F., Ackland, G. J. & Gregoryanz, E. Phonon localization by mass disorder in dense hydrogen-deuterium binary alloy. *Phys. Rev. Lett.* **113**, 175501 (2014).
- Zha, C.-s., Cohen, R. E., Mao, H.-k. & Hemley, R. J. Raman measurements of phase transitions in dense solid hydrogen and deuterium to 325 GPa. *Proc. Natl Acad. Sci. USA* **111**, 4793–4797 (2014).
- McMahon, J. M. & Ceperley, D. M. Ground-state structures of atomic metallic hydrogen. *Phys. Rev. Lett.* **106**, 165302 (2011).
- Azadi, S., Monserrat, B., Foulkes, W. M. C. & Needs, R. J. Dissociation of high-pressure solid molecular hydrogen: a quantum Monte Carlo and anharmonic vibrational study. *Phys. Rev. Lett.* **112**, 165501 (2014).
- Tamblyn, I. & Bonev, S. A. Structure and phase boundaries of compressed liquid hydrogen. *Phys. Rev. Lett.* **104**, 065702 (2010).
- Morales, M., Pierleoni, C., Schwegler, E. & Ceperley, D. M. Evidence for a first-order liquid-liquid transition in high-pressure hydrogen from ab initio simulations. *Proc. Natl Acad. Sci. USA* **107**, 12799–12803 (2010).
- Knudson, M. D. *et al.* Direct observation of an abrupt insulator-to-metal transition in dense liquid deuterium. *Science* **348**, 1455–1460 (2015).

**Acknowledgements** We are grateful to M. Frost for assistance during experiments. This work is supported by a Leadership Fellowship from the UK Engineering and Physical Sciences Research Council (EPSRC), reference number EP/J003999/1. P.D.-S. acknowledges studentship funding from EPSRC grant number EP/G03673X/1.

**Author Contributions** R.T.H. and P.D.-S. carried out the experiments, analysed the data and wrote the paper. E.G. conceived and designed the project, carried out the experiments, analysed the data and wrote the paper.

**Author Information** Reprints and permissions information is available at [www.nature.com/reprints](http://www.nature.com/reprints). The authors declare no competing financial interests. Readers are welcome to comment on the online version of the paper. Correspondence and requests for materials should be addressed to E.G. (e.gregoryanz@ed.ac.uk).

## METHODS

**Sample loadings.** The experimental runs used mostly the same techniques and method described in refs 16, 18, 19 and references therein. For this study we conducted a total of 14 independent experiments up to pressures of  $388 \pm 15$  GPa. In some of the runs we heated the sample, at different pressures, up to temperatures of 465 K. Pressure was generated in long, high-temperature, piston-cylinder diamond anvil cells of our own design equipped with diamonds with culet dimensions ranging from  $30 \mu\text{m}$  to  $15 \mu\text{m}$ . The rhenium foils with thicknesses of  $200\text{--}250 \mu\text{m}$  were used as the gasket material to form the sample chamber. The hydrogen gas was clamped at  $0.175\text{--}0.200$  GPa at 300 K and then further compressed to above 150 GPa, usually within 2–3 h after clamping. The HD was produced by mixing the pure isotopes in gas phases (usually  $<10$  MPa) at 300 K. The partial pressures were used to calculate the composition, which, for the experiment on HD described here, was 75% and 25% for hydrogen and deuterium, respectively (see also ref. 20).

**Optical measurements.** We used 514.15-nm and 647.1-nm excitation wavelengths to collect the spectra. Owing to the quantum efficiency of the visible CCD (charged coupled device) used, the high-energy modes—for example, hydrogen vibrational excitation at above  $3,500 \text{ cm}^{-1}$ —are much weaker than the low-energy lattice modes if probed using a 647.1-nm wavelength. However, in most of the cases, when 514.15-nm excitation is used, the pressure-induced fluorescence from the stressed diamonds obscures the Raman signal, which leaves 647.1-nm excitation as the only available source, as in Fig. 1.

**Pressure and temperature measurements.** For pressure measurements, the stressed-diamond-edge frequency was used and, where applicable, cross-referenced with the frequency of the vibrational modes<sup>19</sup> from previous experiments to maintain self-consistency. An example of how the frequency of the stressed diamond edge was determined, and the dependence of the vibrational frequency of hydrogen versus the frequency of the stressed diamond edge is given in Extended Data Fig. 1a. The first-order diamond Raman band becomes elongated in frequency space, composed of two sharp, well-defined peaks: one corresponding to the stressed culet and the other to the unstressed regions of the diamond. The frequency from the stressed culet was determined by the frequency ( $\omega$ ) at which  $dI/d\omega$  was minimized (where  $I$  is the intensity of the spectrum), a technique proposed in refs 11, 27, and 28.

The calibration data presented in refs 27 and 28 were primarily used here for determining pressure. These two curves agree up to about 200 GPa, but gradually diverge at higher pressures (Extended Data Fig. 2b). For example, at the highest pressure reached, we observed a diamond-edge frequency of  $1,936 \text{ cm}^{-1}$  (see Fig. 1), which corresponds to pressures of approximately 388 GPa and 403 GPa on the scales proposed by Akahama & Kawamura in 2004<sup>27</sup> and 2006<sup>28</sup>, respectively.

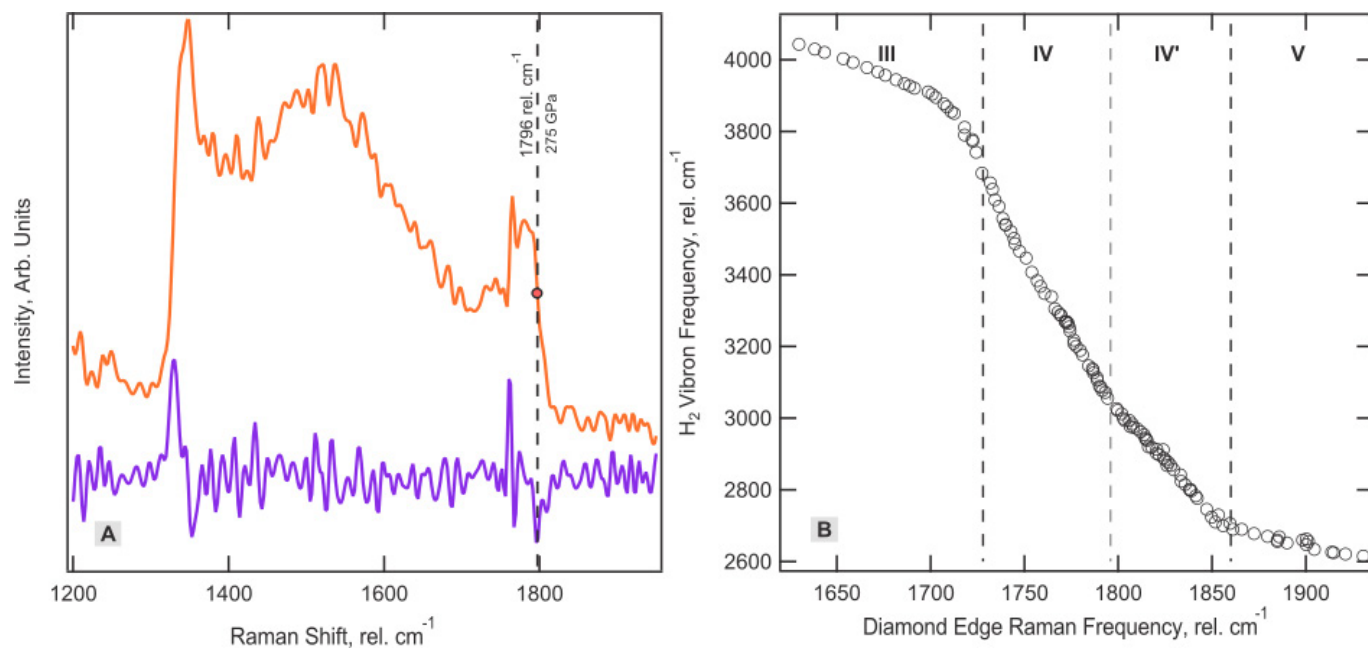
With their latest calibration in 2010<sup>29</sup>, this frequency corresponds to a substantially higher pressure of 449 GPa (Extended Data Fig. 2b). However, the effect of pressures above about 300 GPa on soft samples has yet to be determined; the latest calibration<sup>29</sup> up to 410 GPa needs to be independently verified, particularly for softer samples. To be consistent with previous results, we decided to use the most conservative scale<sup>27</sup>, as was used in our previous studies<sup>16,18,19</sup>. This scale provides a smooth continuation of the frequencies of the low-energy and vibrational modes versus pressure observed by us in all experiments.

We therefore stress that the characteristics that provide evidence for the phase V transition are independent of the choice of the previously discussed calibrations, not a direct consequence. Extended Data Figure 2a demonstrates that the discontinuous change in  $d\nu_1/dP$  for pure  $\text{H}_2$  is present when using any of the stressed-diamond-edge pressure calibrations, and remains just as prominent when using the less-conservative and more-contemporary pressure scales<sup>11,27</sup>.

For heating, we used two custom-built resistive heaters placed around the diamonds and the body of the cell. Temperature was determined using one or two thermocouples, attached to one of the diamonds and/or the gasket.

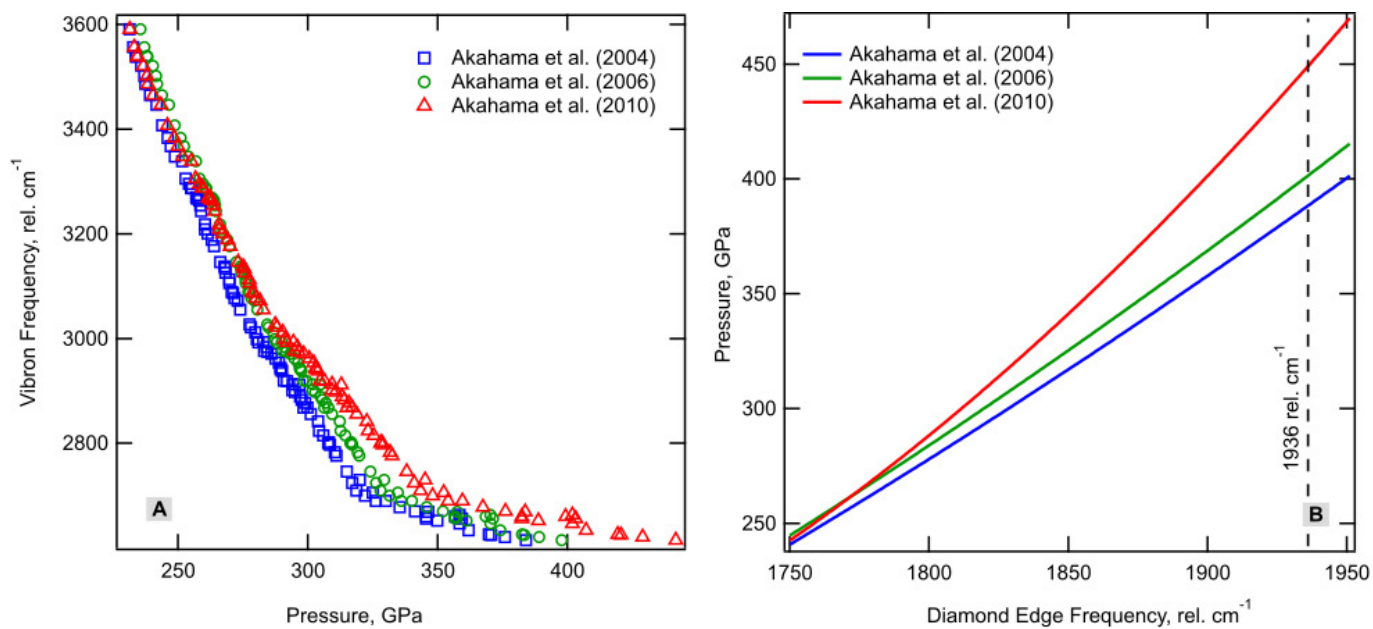
**Calculating relative integrated intensities.** Calculating the relative Raman intensities in the diamond anvil cell is a difficult task, especially when these intensities are of similar magnitude to the relatively low signal-to-noise ratios. Therefore, the data in Fig. 2 are from the spectrum with the highest signal-to-noise ratio in each run. First, the background caused by the pressure-induced fluorescence of the diamond anvils is subtracted. The residual data are then fitted with Voigt profiles, which produces values for the integrated intensities of each excitation. These values are then summed, and the percentage of total Raman activity is calculated; an example is provided in Extended Data Fig. 7. Owing to the extremely small samples, the second-order Raman band also becomes comparable in magnitude to the excitations from the sample (Extended Data Fig. 7, inset). Consequently, at higher pressures for which the  $\nu_1$  excitations overlap with the second-order Raman diamond band, extra care has to be taken. Here, the evolution of the spectra with pressure (which is determined using fits from a previous pressure step as an initial guess) as well as the relationship between the intensity of the first- and second-order diamond bands are used to accurately determine the integrated intensity of  $\nu_1$ .

27. Akahama, Y. & Kawamura, H. High-pressure Raman spectroscopy of diamond anvils to 250 GPa: method for pressure determination in the multimegabar pressure range. *J. Appl. Phys.* **96**, 3748–3751 (2004).
28. Akahama, Y. & Kawamura, H. Pressure calibration of diamond anvil Raman gauge to 310 GPa. *J. Appl. Phys.* **100**, 043516 (2006).
29. Akahama, Y. & Kawamura, H. Pressure calibration of diamond anvil Raman gauge to 410 GPa. *J. Phys. Conf. Ser.* **215**, 012195 (2010).



**Extended Data Figure 1 | Calculating pressure.** a, A typical example of a spectrum from the first-order Raman band of diamond when probing the sample (orange). The frequency edge is given by the vertical dashed line at  $1,796 \text{ rel. cm}^{-1}$ , which corresponds to a pressure of 275 GPa (ref. 27).

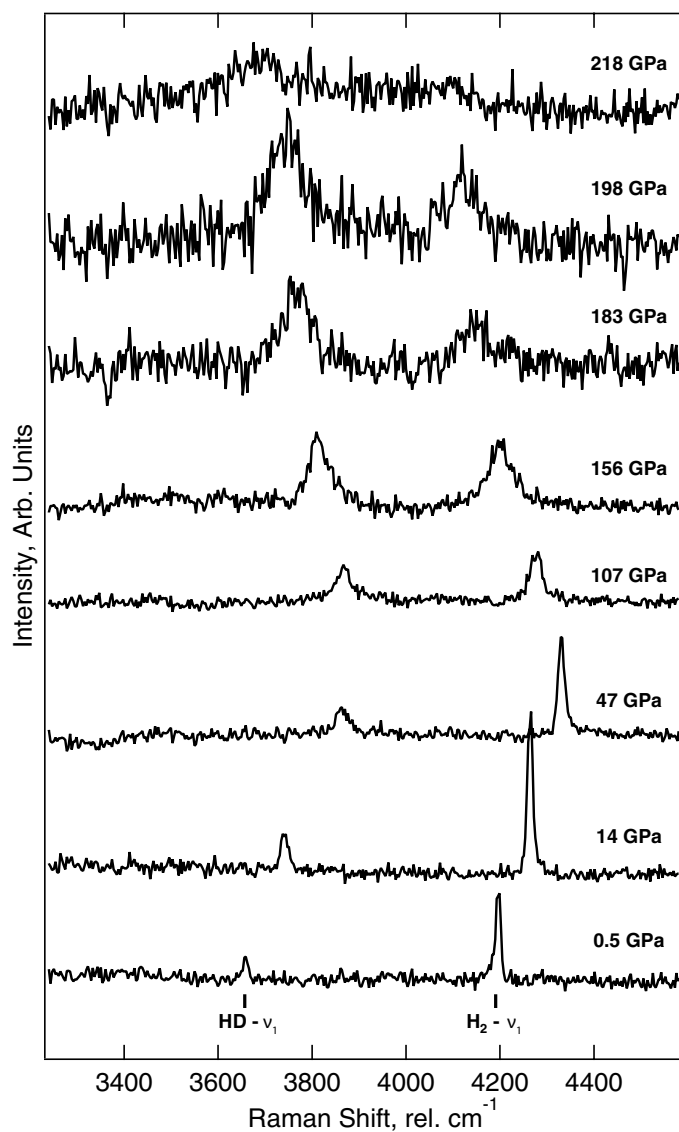
This stressed edge is defined as the frequency that minimizes  $dI/d\omega$  (purple). b, H<sub>2</sub> vibrational-mode (vibron) frequency ( $\nu_1$ ) plotted as a function of the stressed-diamond-edge frequency.



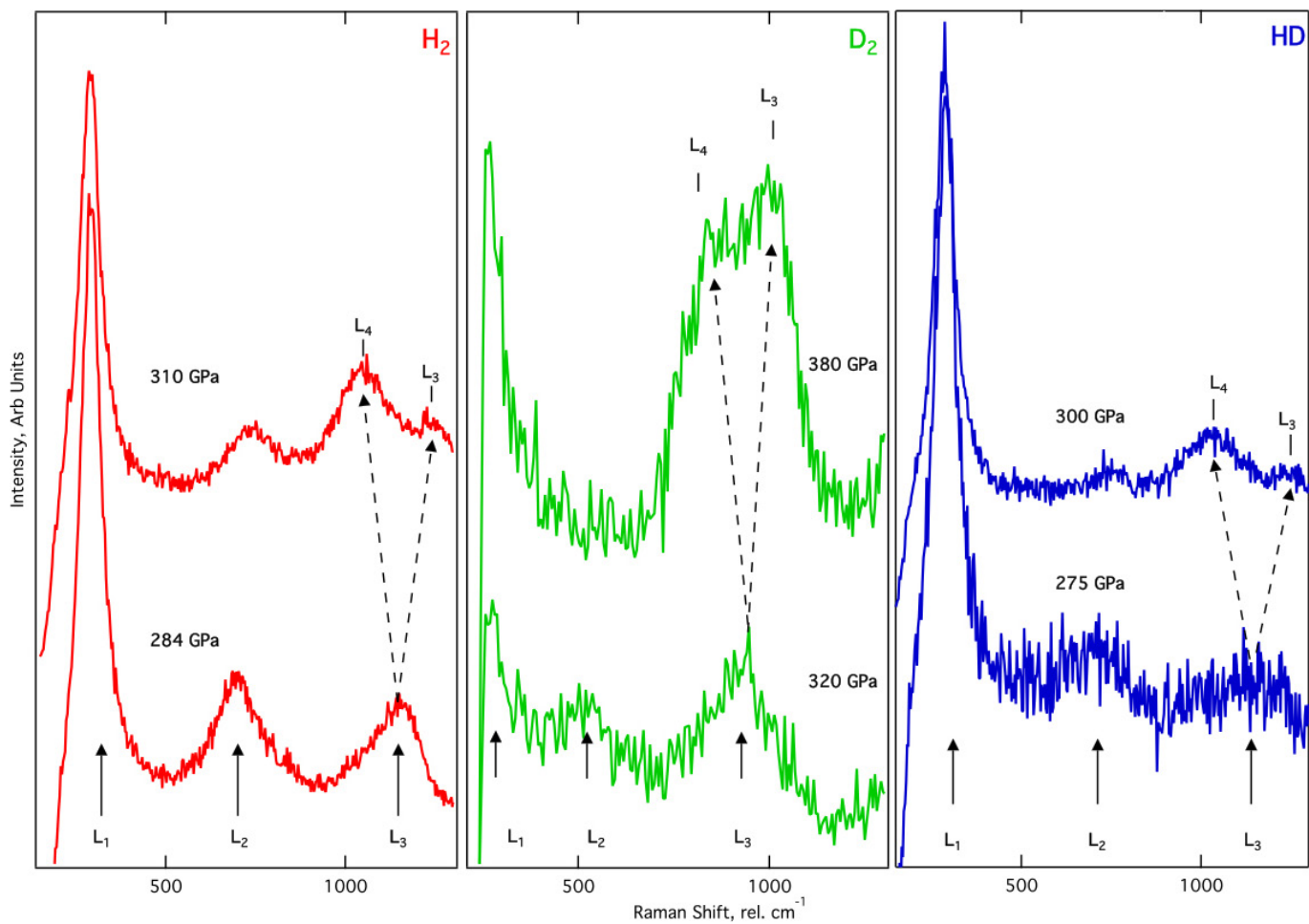
**Extended Data Figure 2 | Comparison of pressure calibrations.**

**a**, Vibration-mode (vibron) frequency plotted using the three pressure gauges of the stressed-diamond frequency proposed by Akahama *et al.*: blue squares<sup>27</sup>, green circles<sup>28</sup> and red triangles<sup>11</sup>. **b**, The three pressure

gauges plotted as a function of pressure, coloured as in **a**; the dashed line marks the highest frequency of the stressed diamond recorded on a HD sample, 1,936 rel.  $\text{cm}^{-1}$ .

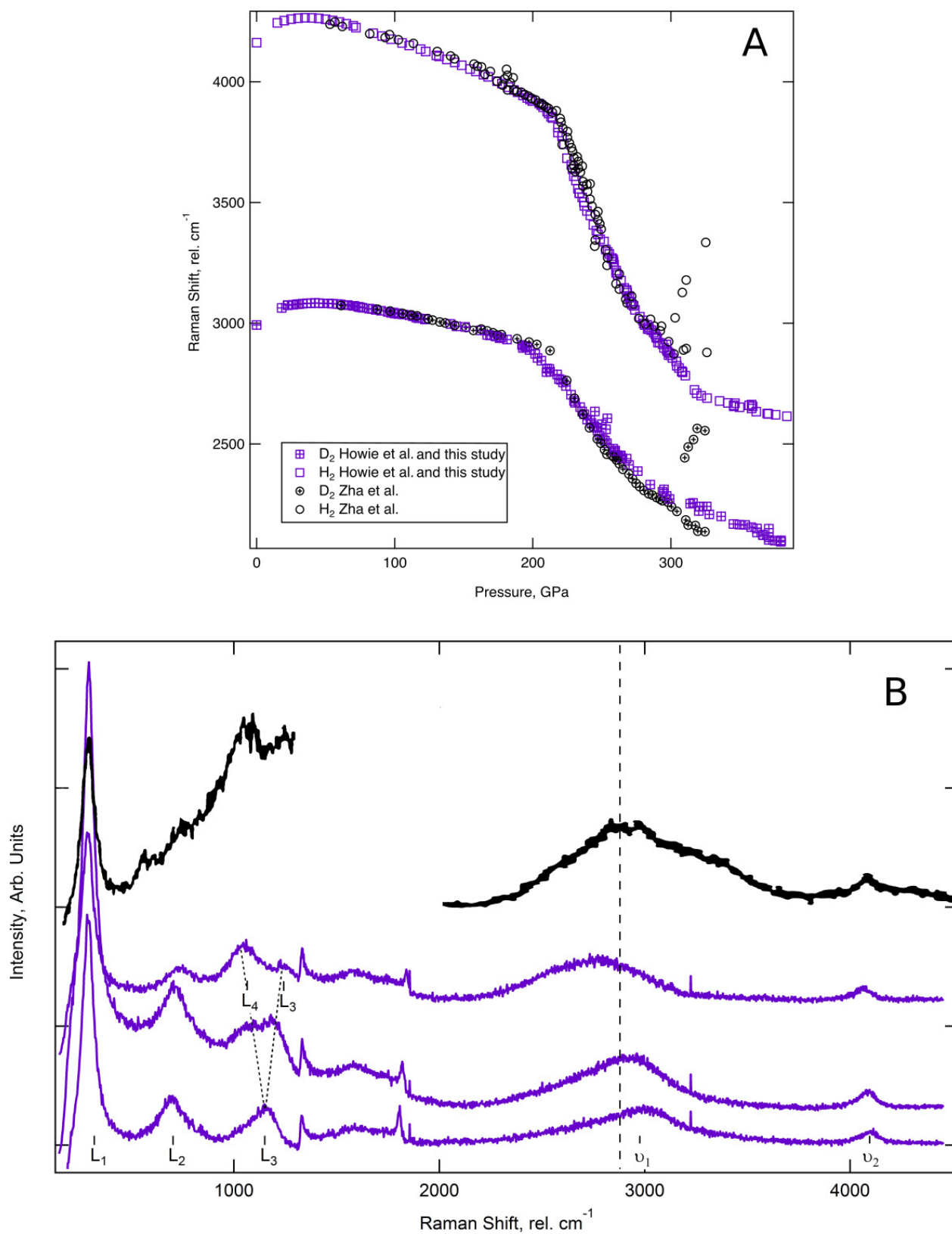


**Extended Data Figure 3 | HD compressed to 218 GPa.** Representative Raman spectra from HD, a mixture of hydrogen (75%) and deuterium (25%), as a function of pressure at 300 K. The spectra show the evolution of the  $\nu_1$  vibrational modes of HD (labelled 'HD- $\nu_1$ ') and  $H_2$  (labelled ' $H_2$ - $\nu_1$ ') from loading at 0.5–218 GPa, as labelled. Above 47 GPa, there is an observed transfer of integrated intensity from the  $\nu_1$  band of  $H_2$  to the  $\nu_1$  band of HD, with the latter vibrational mode becoming stronger than the former at 150 GPa, and the only resolvable  $\nu_1$  band above 218 GPa. The spectra were collected using a 514-nm excitation wavelength. The spectra from this run above 218 GPa are shown in Fig. 1b.



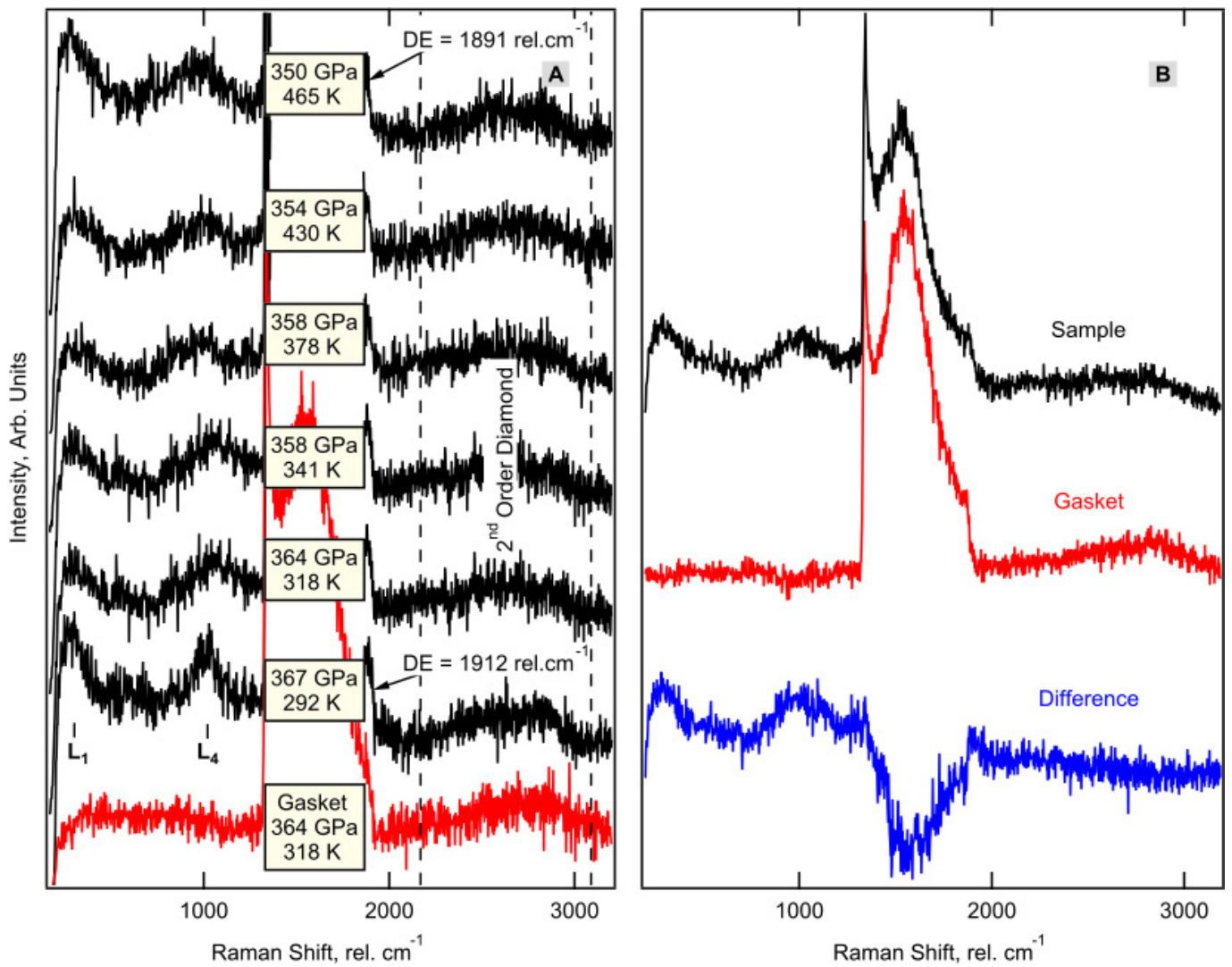
**Extended Data Figure 4 | Low-energy-mode splitting from phase IV to phase IV'.** Representative Raman spectra of the low-frequency excitations of the three isotopes (left, H<sub>2</sub>; centre, D<sub>2</sub>; right, HD) as functions of

pressure during the transition from phase IV to phase IV'. The low-frequency mode L<sub>3</sub> splits to produce mode L<sub>4</sub>.



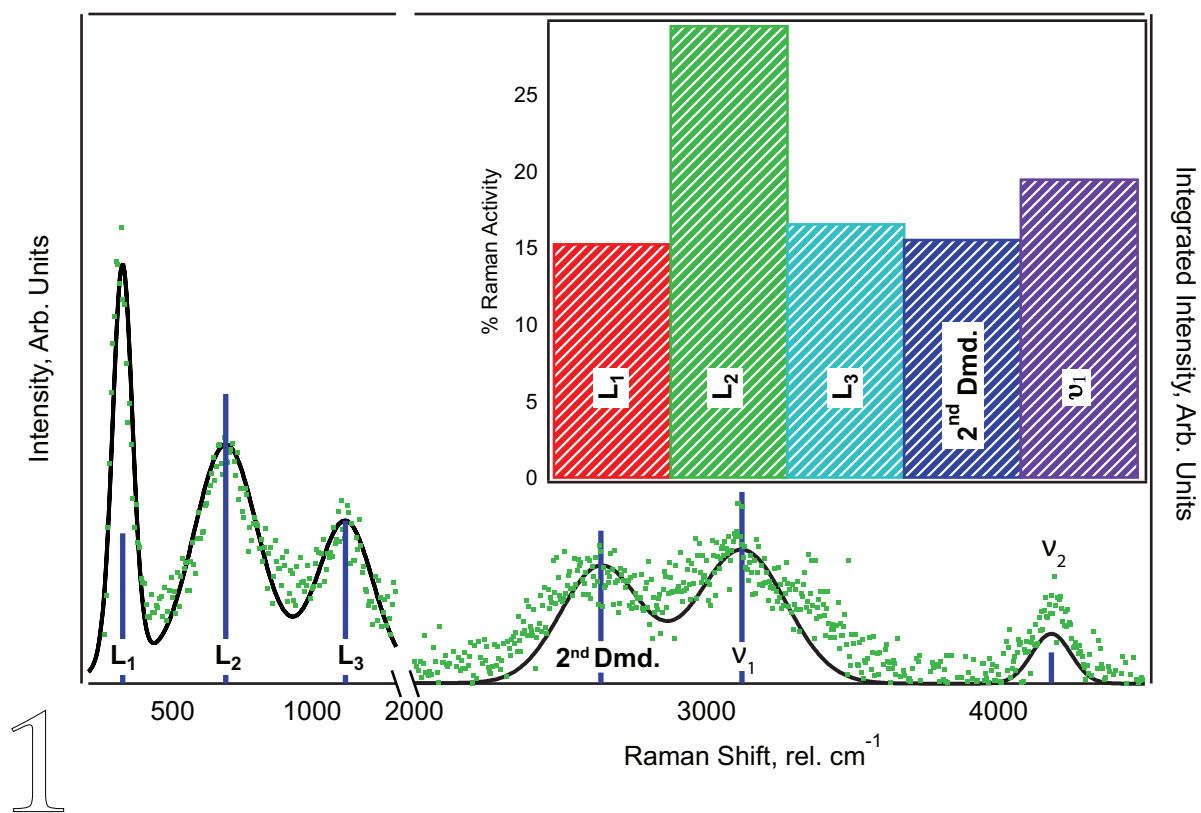
**Extended Data Figure 5 | Comparison with previous data. a**, Frequencies of the vibrational modes versus pressure from ref. 21 (black circles) and the current study and our previous study<sup>16</sup> (violet squares). The open symbols represent data for  $\text{H}_2$ ; the symbols enclosing pluses represent

data for  $\text{D}_2$ . **b**, Representative Raman spectra of hydrogen from ref. 21 (black) and ref. 16 (violet). The dashed vertical line indicates the lowest vibrational-mode frequency (and therefore the highest pressure) observed in ref. 21.



**Extended Data Figure 6 | Heating at about 360 GPa.** **a**, Raman spectra for a pure hydrogen sample, taken using a probe laser with a wavelength of 647 nm, as function of temperature at pressures between 367 GPa and 350 GPa (black). The Raman spectrum collected 2  $\mu\text{m}$  away on the rhenium gasket is shown in red. The vertical dashed lines indicate

the frequency space occupied by the second-order diamond band. DE, diamond edge. **b**, Example spectrum of the sample (black) and the gasket (2  $\mu\text{m}$  away, red), collected at 361 GPa, and the difference between them (blue).



**Extended Data Figure 7 | Calculating relative integrated intensities.** Representative Raman spectrum demonstrating how intensities were calculated for a given spectrum. The best fit (black curve) to the experimental data (green points) is shown (measured by the left axis) along with the integrated intensities for each excitation (indicated by

the height of the blue bars, measured by the right axis). The inset shows the raw value of the integrated intensities of each excitation in the main figure as a percentage of the total Raman activity.  $2^{\text{nd}}$  Dmd., second-order diamond band (unlabelled in the main figure).